International Journal of Nanomedicine

Dovepress
open access to scientific and medical research

Open Access Full Text Article

ORIGINAL RESEARCH

Development of a bone-targeted pH-sensitive liposomal formulation containing doxorubicin: physicochemical characterization, cytotoxicity, and biodistribution evaluation in a mouse model of bone metastasis

This article was published in the following Dove Press journal:
International Journal of Nanomedicine
9 August 2016
Number of times this article has been viewed

Diêgo dos Santos Ferreira,[1,2] Samilla Dornelas Faria,[1] Sávia Caldeira de Araújo Lopes,[1] Cláudia Salviano Teixeira,[1] Angelo Malachias,[3] Rogério Magalhães-Paniago,[3] José Dias de Souza Filho,[4] Bruno Luis de Jesus Pinto Oliveira,[2] Alexander Ramos Guimarães,[2] Peter Caravan,[2] Lucas Antônio Miranda Ferreira,[1] Ricardo José Alves,[1] Mônica Cristina Oliveira[1]

[1]Department of Pharmaceutical Products, Faculty of Pharmacy, Universidade Federal de Minas Gerais, Belo Horizonte, Minas Gerais, Brazil; [2]Athinoula A Martinos Center for Biomedical Imaging, Massachusetts General Hospital, Harvard Medical School, Boston, MA, USA; [3]Department of Physics, [4]Department of Chemistry, Institute of Exact Sciences, Universidade Federal de Minas Gerais, Belo Horizonte, Brazil

Correspondence: Mônica Cristina Oliveira
Department of Pharmaceutical Products, Faculty of Pharmacy, Universidade Federal de Minas Gerais, 6627 Avenida Antônio Carlos, Belo Horizonte, Minas Gerais 31270-901, Brazil
Tel +55 31 3409 6945
Fax +55 31 3409 6935
Email monicacristina@ufmg.br

Background: Despite recent advances in cancer therapy, the treatment of bone tumors remains a major challenge. A possible underlying hypothesis, limitation, and unmet need may be the inability of therapeutics to penetrate into dense bone mineral, which can lead to poor efficacy and high toxicity, due to drug uptake in healthy organs. The development of nanostructured formulations with high affinity for bone could be an interesting approach to overcome these challenges.

Purpose: To develop a liposomal formulation with high affinity for hydroxyapatite and the ability to release doxorubicin (DOX) in an acidic environment for future application as a tool for treatment of bone metastases.

Materials and methods: Liposomes were prepared by thin-film lipid hydration, followed by extrusion and the sulfate gradient-encapsulation method. Liposomes were characterized by average diameter, ζ-potential, encapsulation percentage, X-ray diffraction, and differential scanning calorimetry. Release studies in buffer (pH 7.4 or 5), plasma, and serum, as well as hydroxyapatite-affinity in vitro analysis were performed. Cytotoxicity was evaluated by MTT assay against the MDA-MB-231 cell line, and biodistribution was assessed in bone metastasis-bearing animals.

Results: Liposomes presented suitable diameter (~170 nm), DOX encapsulation (~2 mg/mL), controlled release, and good plasma and serum stability. The existence of interactions between DOX and the lipid bilayer was proved through differential scanning calorimetry and small-angle X-ray scattering. DOX release was faster when the pH was in the range of a tumor than at physiological pH. The bone-targeted formulation showed a strong affinity for hydroxyapatite. The encapsulation of DOX did not interfere in its intrinsic cytotoxicity against the MDA-MB-231 cell line. Biodistribution studies demonstrated high affinity of this formulation for tumors and reduction of uptake in the heart.

Conclusion: These results suggest that bone-targeted pH-sensitive liposomes containing DOX can be an interesting strategy for selectively delivering this drug into bone-tumor sites, increasing its activity, and reducing DOX-related toxicity.

Keywords: hydroxyapatite-targeted formulations, bisphosphonates, pH-responsive nanostructures, bone-tumor treatment

Introduction

Around 60%–75% of breast metastases occur in bones.[1–3] These metastatic diseases, characterized by increased osteoclastic activity and osteolysis, are associated with

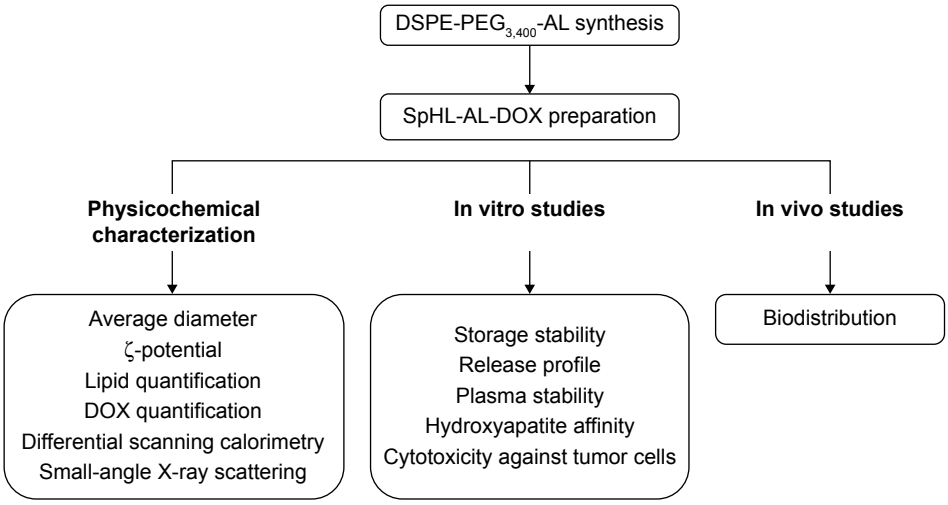

Figure 1 Flowchart containing the experiments performed in this study.
Abbreviations: DSPE, 1,2-distearoyl-*sn*-glycero-3-phosphoethanolamine; PEG, polyethylene glycol; SpHL, pH-sensitive liposomes; AL, alendronate; DOX, doxorubicin.

pain, fractures, and nerve-compression syndromes, which result in decreased quality of life.[2,3] Currently, there is no curative treatment for bone tumors. In this context, effective therapies to inhibit the progression of bone metastases would have important clinical benefits.

A major characteristic of bone is its high content of the mineral hydroxyapatite (HA). This feature limits the diffusion of drugs into the bone, and prevents access to less vascularized areas.[4] Among the drugs able to accumulate in bones, the bisphosphonates have been studied as targeting moieties through the chemical modification of nonspecific bone-therapeutic agents or binding to the surface of drug-delivery systems, including liposomes.[5–10] The ability of bisphosphonates to accumulate in bones is explained by their similarity to pyrophosphate, a natural antimineralization agent. The bisphosphonates possess a P–C–P backbone, which presents a bidentate ligand able to complex calcium ions present in HA.[11]

In spite of the high affinity of bisphosphonate-attached liposomes for HA, it is well known that liposomal formulations may present a slow release of the internal content and be unable to fuse with the tumor cell membrane, hindering the intracellular uptake of drugs. In order to overcome these limitations, pH-sensitive liposomes have been developed. These liposomes have been designed to undergo destabilization when submitted to acidic environments, as occurs in the tumor extracellular matrix as well as within the endosomes.[12]

In this study, we describe the preparation of novel alendronate-coated long-circulating pH-sensitive liposomes containing doxorubicin (SpHL-AL-DOX). The pH sensitivity is reached due to the presence of the lipids 1,2-dioleoyl-glycero-3-phosphatidylethanolamine (DOPE) and cholesteryl hemisuccinate (CHEMS), while the bone targeting is provided by the presence of 1,2-distearoyl-*sn*-glycero-3-phosphoethanolamine-*N*-(AL-[polyethylene glycol]-3,400) (DSPE-$PEG_{3,400}$-AL). The PEG is used as both a spacer to extend the AL residue out of the liposomal bilayer and an agent to avoid liposomal uptake by the mononuclear phagocytic system, and consequently to increase the circulation time.[13] This formulation can potentially be applied for the treatment of bone metastases. It is anticipated that the bone selectivity of SpHL-AL-DOX can lead to locally high concentrations of DOX and enhance its therapeutic effect. In addition, reduction of cardiac DOX uptake and decreased cardiotoxicity are the potential major benefits that can be achieved with this targeting approach. Here, we developed and evaluated the physicochemical characteristics of SpHL-AL-DOX and the effects of the presence of AL on drug release, plasma stability, and affinity for HA. In vitro cytotoxicity studies were also performed to demonstrate the maintenance of the efficacy of the encapsulated DOX against tumor cells when compared to the free drug. A flowchart of the experiments performed is presented in Figure 1.

Materials and methods

Materials

DOPE and DSPE-$PEG_{2,000}$ were supplied by Lipoid GmbH (Ludwigshafen, Germany). DSPE-$PEG_{3,400}$-*N*-(*N*-hydroxysuccinimide) (DSPE-$PEG_{3,400}$-NHS) was purchased from NanoCS (New York, NY, USA). CHEMS, sodium AL, DOX, 4-(2-hydroxyethyl)-1-piperazineethanesulfonic

acid (HEPES) sodium salt, magnesium chloride, sodium chloride, sodium hydroxide, Triton X-100, sodium dodecyl sulfate, 3-(4,5 dimethylthiazolyl-2)-2,5-diphenyltetrazolium bromide (MTT), fetal bovine serum, penicillin, and streptomycin were obtained from Sigma-Aldrich Co. (St Louis, MO, USA). Dulbecco's Modified Eagle's Medium was purchased from Thermo Fisher Scientific (Waltham, MA, USA). Dimethyl sulfoxide (DMSO) and ethanol were obtained from Thermo Fisher Scientific. All other chemicals used in this study were of analytical grade. The human breast adenocarcinoma cell line (MDA-MB-231) was purchased from the American Type Culture Collection (Manassas, VA, USA).

Synthesis of DSPE-PEG$_{3,400}$-AL

DSPE-PEG-NHS (20 mg, 4.5 µmol) was dissolved in DMSO (0.5 mL), and then a solution of sodium AL (10 mg, 30.8 µmol) and sodium hydroxide (3.7 mg, 92.2 µmol) in DMSO (0.5 mL) was added. The reaction mixture was stirred for 12 hours at room temperature, and then transferred to a cellulose-membrane tube (CelluSep; molecular weight cutoff [MWCO] 7,000 kDa). The sample was dialyzed sequentially in 50 mmol·L^{-1} NaCl solution (twice, 1,000 mL, 6 hours each) and distilled water (twice, 1,000 mL, 6 hours each). To obtain the final product (DSPE-PEG$_{3,400}$-AL), the dialyzed solution was freeze-dried. The scheme of the reaction is shown in Figure 2. The infrared (IR), ^{1}H, and ^{31}P nuclear magnetic resonance (NMR) spectra of the reagents and products were obtained (Supplementary materials). In addition, the phosphorus concentration in the reagents and product was measured by inductively coupled plasma mass spectrometry (ICP-MS) in an 8800 ICP-QQQQ (Agilent Technologies, Santa Clara, CA, USA).

Liposome preparation

SpHL-AL-DOX were prepared by thin-film hydration followed by extrusion and DOX encapsulation by remote loading, driven by a transmembrane sulfate gradient.[14,15] Briefly, DOPE, CHEMS, and DSPE-PEG$_{3,400}$-AL in a 5.7:3.8:0.5 molar ratio, respectively, were dissolved in chloroform and evaporated under reduced pressure until a thin lipid film was obtained. The resulting film was hydrated with ammonium sulfate solution (300 mmol·L^{-1}, pH 7.4) to reach 10 mmol·L^{-1} total lipid concentration. The liposomes were then sequentially extruded (Lipex® biomembrane extruder; Northern Lipids, Burnaby, BC, Canada) through a series of polycarbonate membranes with pore sizes of 0.4, 0.2, and 0.1 µm (five cycles for each). The external medium was eliminated by ultracentrifugation (Optima® L-80XP; Beckman Coulter, Pasadena, CA, USA) at 150,000× *g* at 4°C for 90 minutes. The pellet was resuspended in HEPES-buffered saline (HBS), pH 7.4. This formulation was incubated with DOX (2 mg·mL^{-1}) for 12 hours at 4°C. Unentrapped DOX was eliminated by ultracentrifugation at 150,000× *g* at 10°C for 90 minutes. Also prepared as aforementioned procedure were AL-uncoated SpHL-DOX consisting of DOPE, CHEMS, and DSPE-PEG$_{2,000}$ in a 5.7:3.8:0.5 molar ratio, respectively, as well as SpHL-AL and SpHLs without DOX.

Liposome characterization

The liposomes were characterized by their encapsulation percentage (EP), drug:lipid ratio, size, ζ-potential, and

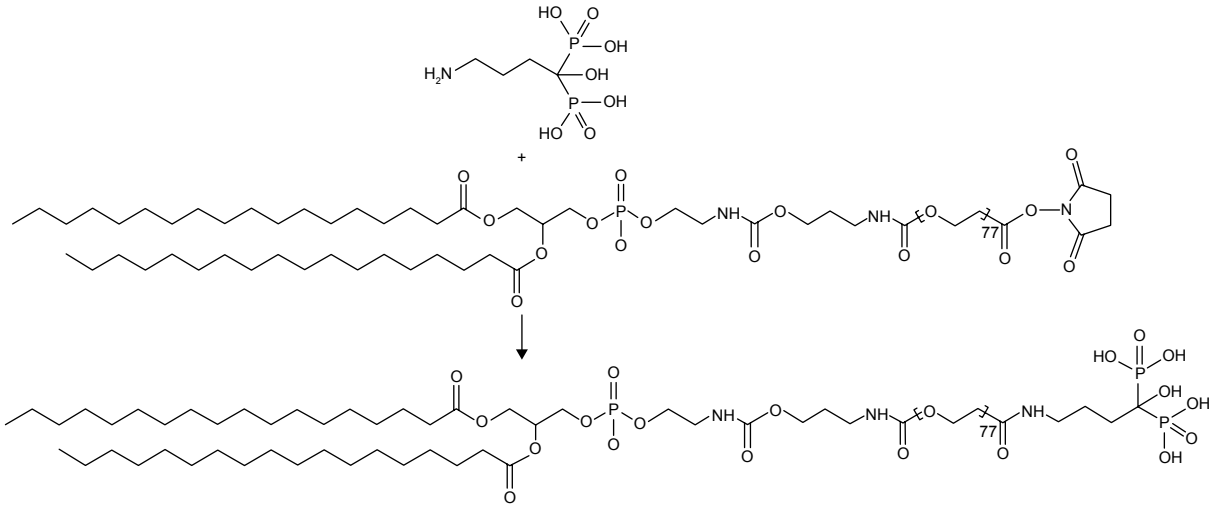

Figure 2 Schematic representation of reaction between sodium AL and DSPE-PEG$_{3,400}$-NHS to produce DSPE-PEG$_{3,400}$-AL.
Abbreviations: AL, alendronate; DSPE-PEG$_{3,400}$-NHS, 1,2-distearoyl-*sn*-glycero-3-phosphoethanolamine-*N*-(*N*-hydroxysuccinimide-[polyethylene glycol]-3,400).

polydispersity index (PDI). The EP of DOX in the liposomes was determined by high-performance liquid chromatography (HPLC). Equipment parameters are described in Supplementary materials. The amount of DOX was determined in the liposomes before ultracentrifugation (unpurified liposomes) and after ultracentrifugation (purified liposomes). For disruption of the liposomes, an aliquot of 100 µL of the formulation was taken and diluted to 1 mL using methanol. The theoretical concentrations of DOX and lipids were equal to 200 $\mu g \cdot mL^{-1}$ and 1 $mmol \cdot L^{-1}$, respectively. These mixtures were diluted with the mobile phase to theoretical concentrations of DOX equal to 40 $ng \cdot mL^{-1}$ and lipids equal to 200 $nmol \cdot L^{-1}$ before HPLC analysis.

The lipid content was determined by measurement of the phosphorus concentration in the liposomal dispersion by means of ICP-MS (8800 ICP-QQQQ), and the drug:lipid ratio ($mol \cdot mol^{-1}$) and DOX content (% weight) were calculated. The average diameter and PDI of the vesicles were determined by quasielastic light scattering at 25°C and a 90° angle using monomodal analysis. The ζ-potential was evaluated by determining the electrophoretic mobility at an angle of 90°. All samples were diluted in HBS pH 7.4, and the measurements were performed in triplicate using a Zetasizer analyzer (3000HS; Malvern Instruments, Malvern, UK).

Storage stability

In order to evaluate the shelf life of SpHL-AL, the samples were stored under N_2 atmosphere at 4°C. An aliquot of the sample was removed at different time intervals to measure the average diameter, ζ-potential, and PDI, as described earlier.

Differential scanning calorimetry and small-angle X-ray scattering

Calorimetric analyses of liposome constituents (Table S1) were performed using differential scanning calorimetry (DSC; model 2910; TA Instruments, New Castle, DE, USA). Methodological details are described in Supplementary materials. Samples submitted to DSC analysis were also submitted to small-angle X-ray scattering (SAXS) analysis at variable temperatures, according to the methodology described in Supplementary materials. Temperatures for SAXS analyses were chosen based on the DSC curve of each sample. Temperature points before, between, and after subsequent DSC peaks were chosen in order to verify the alterations in structural organization caused by the calorimetric events.

In vitro drug release in buffer, serum, and plasma

The in vitro DOX release from SpHL-AL-DOX or SpHL-DOX was assessed in HBS at pH 7.4 or pH 5. One milliliter of SpHL-AL-DOX or SpHL-DOX (pH 7.4 or 5) was transferred to a cellulose-membrane tube (CelluSep, MWCO 10,000 kDa). The dialysis membrane was then placed in the dialysis medium (100 mL) and gently shaken at 22°C. At several time intervals, 50 µL of external buffer solution was withdrawn and replaced with an equal volume of fresh medium. The concentration of DOX in the dialysis medium and in liposomes after dialysis was determined by HPLC analysis (Supplementary materials). The percentage of DOX released was calculated by dividing the amount of DOX in the dialysis medium by the amount of DOX added in the dialysis sac. The average diameter and PDI of formulations used in the studies at pH 7.4 were determined prior to and after the experiment. Release studies in plasma and serum were also performed. Liposomes were diluted in plasma or serum ($1:4\ v \cdot v^{-1}$) prior to transfer to the cellulose-membrane tubes. Dialysis was performed at 37°C, as described earlier.

In vitro assessment of HA-binding affinity

HA nanopowder was suspended in HBS pH 7.4 ($10\ mg \cdot mL^{-1}$). SpHL-AL-DOX or SpHL-DOX was poured onto HA suspensions (final concentration of lipids 1.7 $\mu mol \cdot L^{-1}$), and the mixture was then gently shaken at room temperature. At several time points, the samples were centrifuged at 5,000× *g* for 15 minutes. The supernatant was collected, and the concentration of phosphorus in the sample measured by ICP-MS. Samples of HA nanopowder, SpHL-AL-DOX, or SpHL-DOX alone were submitted to the same protocol, and the phosphorus concentration was also measured by ICP-MS. It was not possible to quantify any significant amount of phosphorus in the supernatant of the samples containing only HA nanopowder. The phosphorus concentration measured in the supernatant of the samples containing SpHL-AL-DOX or SpHL-DOX alone was considered to reflect the unbounded concentration. To evaluate the release of the bound SpHL-AL-DOX from HA, the pellet of the sample centrifuged at 6 hours was resuspended in HBS pH 7.4, and at several time intervals (up to 24 hours) the sample was centrifuged at 5,000× *g* for 15 minutes. The supernatant was collected, and the concentration of phosphorus in the sample was measured by ICP-MS. Once again, the HA nanopowder was submitted to the same protocol and the phosphorus concentration in the supernatant measured, in order to demonstrate absence of interference of HA on the quantification of liposomal phosphorus.

Cytotoxicity assay

The human breast cancer cell line MDA-MB-231 was cultured in Dulbecco's Modified Eagle's Medium supplemented with 10% fetal bovine serum, penicillin (100 IU·mL^{-1}), and streptomycin (100 mg·mL^{-1}). The cells were maintained at 37°C in a humidified 5% CO_2 atmosphere. An aliquot containing 3×10^3 cells was distributed in 96-well plates. After 24 hours of growth, the cells were submitted to treatment with free DOX, SpHL-AL-DOX, and SpHLs. The DOX-concentration range varied between 1 and 500 mmol·L^{-1}. Forty-eight hours after the initial treatment, cell viability was assessed by MTT reduction. First, 100 µL of a 0.5 mg/mL MTT solution was added to each well of the plate. After 2 hours, MTT crystals were solubilized in 100 µL of sodium dodecyl sulfate 10% (w/v) dissolved in 0.1 mmol·L^{-1} HCl solution. Cell viability was estimated by measuring the rate of mitochondrial reduction of MTT, determined by evaluating the absorbance of the converted dye at a wavelength of 595 nm. Absorbance values of the wells in which the cells were maintained in medium alone were considered to have a cell viability of 100%. Cells treated with SpHLs were used as a control group. Data are expressed as percentage of cell viability compared to this control group (mean ± standard deviation). The half-maximal inhibitory concentration (IC_{50}) values of free DOX and SpHL-AL-DOX were calculated using GraphPad Prism 5.0 (GraphPad Software, San Diego, CA, USA). At least three independent experiments were performed.

Biodistribution studies

Biodistribution studies were performed according to and ethically approved by the experimental guidelines of the Animal Experimentation Ethics Committee of Massachusetts General Hospital Subcommittee on Research Animal Care (protocol 2014N000026). Female nude BALB/c mice bearing MDA-MB-231 bone metastases were employed in this study. Tumor-bearing mice were established as follows: 10^5 MDA-MB-231 cells were inoculated into the medullar channel of the left tibia of the mice. Tumors were allowed to grow for 15 days. Presence of tumors was confirmed by histological and bone-scintigraphy analyses (data not shown).

After tumor growth, animals were intravenously injected with free DOX, SpHL-DOX, or SpHL-AL-DOX (15 mg·kg^{-1}, n=6 each group) and killed after 2 hours (n=3) or 8 hours (n=3). Blood, liver, spleen, heart, kidney, and tumor samples were collected for quantification of DOX by HPLC. Blood was collected in heparinized tubes and centrifuged at 2,000× *g* for 10 minutes. To preserve DOX from degradation, all samples were stored at –20°C until analysis. Methodological details about the quantification are described in Supplementary materials.

Results and discussion

Synthesis of DSPE-$PEG_{3,400}$-AL

By comparing the DSPE-$PEG_{3,400}$-AL to DSPE-$PEG_{3,400}$-NHS IR spectra, elimination of the peak at 1,712 cm^{-1} was observed, which was related to the presence of the NHS group (Figure S1). The elimination of the NHS group occurred due to the nucleophilic attack of the amine groups of sodium AL on the NHS-activated carbonyl group from DSPE-$PEG_{3,400}$-NHS. Similar results have been previously demonstrated by Baki. For ^{1}H NMR of sodium AL (Figure S2), it was possible to observe two signals of chemical shifts at 2.01 and 3.04 parts per million (ppm), with integrals equal to 4 and 2, respectively. These signals were related to the hydrogen atoms of the aliphatic chain of the AL molecule. ^{1}H NMR of the DSPE-$PEG_{3,400}$-NHS (Figure S3) showed an intense singlet at 3.61 ppm (ethylene glycol), a group of multiplets between 1.2 and 1.3 ppm (two lateral stearyl chains), a triplet at 0.79 ppm (two groups, $–CH_3$ terminal), and a singlet at 2.69 (NHS group). ^{1}H NMR of the DSPE-$PEG_{3,400}$-AL (Figure S4) revealed reduction of the signal relative to the NHS group and the presence of two signals at 1.92 and 2.95 ppm, which were related to insertion of the AL molecule in the DSPE-$PEG_{3,400}$-NHS. From the ^{31}P NMR of DSPE-$PEG_{3,400}$-AL (Figure S5), two sharp peaks were observed at 17.76 and 0.07 ppm, representing the coexistence of phosphonate and phosphate groups, respectively, in the same molecule.[16,17] In addition, the measurement of the amount of phosphorus by means of ICP-MS showed an increase of 24.24% in DSPE-$PEG_{3,400}$-AL compared to the DSPE-$PEG_{3,400}$-NHS sample (Table 1). Therefore, these findings strongly suggest attachment of the AL molecule to DSPE-$PEG_{3,400}$-NHS.

The low reaction yield (~24%) must have been related to the hydrolysis of DSPE-PEG-NHS caused by residual water

Table 1 Phosphorus concentration of lipid samples submitted to ICP-MS analyses

Sample	P expected (ppb)	P observed (ppb)
DSPE-$PEG_{3,400}$-NHS	53.16	49.93
DSPE-$PEG_{3,400}$-AL	152.41 for yield equal to 100% 49.14 for yield equal to 0	74.17

Abbreviations: ICP-MS, inductively coupled plasma mass spectrometry; DSPE-$PEG_{3,400}$-NHS, 1,2-distearoyl-*sn*-glycero-3-phosphoethanolamine-*N*-(*N*-hydroxysuccinimide-[polyethylene glycol]-3,400); AL, alendronate; ppb, parts per billion.

molecules present in the solvent bulk prior to the reaction with AL.[18] This would cause elimination of the NHS group and inactivation of the carboxyl group, which would be less susceptible to the nucleophilic attack by the amino group of AL molecules. This theory is supported by the results found in ^{1}H NMR and IR spectra, which showed complete elimination of NHS-associated signals.

Liposome characterization

The physicochemical properties of the liposomal formulations are shown in Table 2. The average size of all liposomal preparations varied, ranging from 150 to 185 nm. The encapsulation of DOX into SpHLs or SpHL-AL led to the formation of liposomes of similar size. It is well known that liposomal preparations for anticancer treatment must present small vesicles to comply with safety requirements and improve therapeutic efficacy.[19] Since tumor sites possess a leaky vasculature, liposomes must be of adequate size to deliver anticancer agents by means of the enhanced permeability and retention (EPR) effect. This effect occurs due to the anatomic differences between normal and cancerous tissue, since capillaries in the tumor area possess increased permeability. This defective vascular architecture, coupled with poor lymphatic drainage, induces EPR. Therefore, liposomes smaller than 200 nm have been shown to accumulate preferentially in tumors, due to this EPR effect. Moreover, it is important to note that the size range is a compromise between the loading efficiency of liposomes (increases with increasing size), liposome stability (decreases with increasing size above an optimal 80–200 nm range), and ability for uptake in the tumors (decreases with increasing size).[20–22] PDI values of the formulations varied from 0.1 to 0.15, which means that the formulations were homogeneously dispersed.

As for ζ-potential, it was more negative for SpHL-AL-DOX compared to SpHL-DOX (−12.4 mV vs −7.1 mV). Although no statistical difference was observed for the ζ-potentials of the SpHL (−5.4 mV) or SpHL-AL (−10.6 mV) samples, a tendency toward more negative values was observed for SpHL-AL. These findings strongly suggest the presence of AL molecules on the surface of liposomes. AL contains two phosphonate groups, whose pKa values are 1.33, 2.16–2.72, 5.95–8.73, and 10.25–11.07, which means that at neutral pH, at least two hydroxyl groups are deprotonated.[23] Besides that, management of the ζ-potential is important to guarantee adequate shelf-life stability. In general, the higher the ζ-potential absolute value, the more physically stable the liposomal formulations. This occurs because the aggregation of the particles is less likely to occur, due to electrical repulsion forces.[24]

EP was around 75% and 95% for SpHL-DOX and SpHL-AL-DOX, respectively. The increase in EP for SpHL-AL-DOX may have been due to electrostatic interactions between the phosphate group of AL molecules and the amino group of DOX molecules. These interactions were demonstrated by SAXS studies. The yield of recuperation of phospholipids after liposome purification was typically around 80%, as determined by phosphorus ICP-MS. Drug content, when measured by weight percentage, varied between 20% and 25% of the total. Considering the higher entrapment of DOX in SpHL-AL-DOX, a higher drug:lipid ratio was found compared to SpHL-DOX.

Storage stability

The mean diameter, PDI, and ζ-potential of SpHL-AL stored at 4°C were studied over a time course of 4 months (Table 3). The choice of this formulation was based on two aspects: 1) the encapsulation of DOX into the liposomes was nearly complete through the incubation of the drug with these blank liposomes, and 2) DOX possesses low stability in an aqueous solution, even if stored at a low temperature.[25] Therefore, it would be interesting to prepare stable blank liposomes to encapsulate the drug shortly before use.

A typical phenomenon of instability of the liposomal formulation is an increase in particle size, due to the aggregation

Table 2 Physicochemical properties of the liposomal formulations

Formulation	Size (nm)	PDI	ζ-potential (mV)	EP (%)	Phospholipid content[a] (nmol·L^{-1})	DOX content (weight %)	Drug:lipid ratio (mol·mol^{-1})
SpHLs	141±15	0.12±0.06	−5.4±2.2	–	–	–	–
SpHL-DOX	151±10	0.10±0.08	−7.1±0.7	74.5±6.3	4.78±0.23	21.4±1.9	0.33±0.03
SpHL-AL	183±19*	0.15±0.04	−10.6±4.4	–	–		–
SpHL-AL-DOX	168±24	0.11±0.04	−12.4±3.0*	94.7±7.7	4.97±0.09	24.9±2.1	0.40±0.03*

Notes: *Significant differences between SpHL-AL or SpHL-AL-DOX and their respective AL-uncoated formulations (SpHLs and SpHL-DOX, respectively), as assessed by one-way ANOVA followed by Tukey's HSD test ($P<0.05$); [a]theoretical concentration of phospholipids equal to 6.2 nmol·L^{-1}. Values expressed as mean ± SD (n=3).
Abbreviations: PDI, polydispersity index; EP, encapsulation percentage; DOX, doxorubicin; SpHLs, pH-sensitive liposomes (long-circulating); AL, alendronate; ANOVA, analysis of variance; HSD, honest significant difference; SD, standard deviation.

Table 3 Physicochemical stability of SpHL-AL

Time (days)	Size (nm)	PDI	ζ-Potential (mV)
0	154±4*	0.11±0.03	−10.6±20.4
7	164±3	0.12±0.01	−10.1±0.8
14	162±2	0.10±0.02	−11.1±1.5
21	159±2	0.11±0.01	−11.3±1.2
30	162±3	0.11±0.02	−10.9±0.3
60	162±2	0.09±0.01	−9.2±1.5
90	160±2	0.10±0.04	−10±1.7
120	166±2	0.10±0.03	−10.6±0.4

Notes: *The only significant statistical difference noticed in this experiment was for the mean diameter value of SpHL-AL at day 0 when compared to any other time interval. For the other time points or parameters (PDI and ζ-potential), no statistical difference was observed. These analyses were realized by one-way ANOVA followed by Tukey's HSD test ($P<0.05$). Values expressed as mean ± SD (n=3).

Abbreviations: SpHL-AL, alendronate-coated pH-sensitive liposomes (long-circulating, without doxorubicin); PDI, polydispersity index; ANOVA, analysis of variance; HSD, honest significant difference; SD, standard deviation.

or fusion of liposomes upon storage. An increase in particle size of liposomes generally results in rapid uptake by mononuclear phagocyte system, with a subsequent rapid clearance and a short half life. Moreover, the fusion of vesicles leads to the leakage of the encapsulated drug and changes the surface charge. Therefore, controlling and maintaining small liposomes of uniform size are critical in developing a viable pharmaceutical product.[18] The mean diameter varied from 154 to 166 nm during the first storage week. After that, the values of size, PDI, and ζ-potential remained constant, indicating good stability of the formulation. The maintenance of the mean diameter over time may have been due to the highly negative surface charge and the presence of PEG chains on the liposome surface, which could have prevented vesicle aggregation through steric repulsion, improving the stability of the formulations.[26,27] These results are in agreement with those previously reported by Lopes et al, using a similar liposomal composition.[28]

DSC and SAXS analysis

Mixtures of all the lipids used in the formulation were submitted to DSC and SAXS analysis. For the mixture DOPE:HBS, three endothermic peaks centered at −25°C, −3°C, and 12°C were observed in DSC curves (Figure 3A). The intense peak observed at −3°C can be attributed to the ice melting, as previously described by Lopes et al.[29] SAXS patterns for the DOPE:HBS sample recorded at different temperatures are presented in Figure 3B. Diffraction patterns of DOPE at −30°C and −18°C showed SAXS peaks at q=1.138, 2.270, and 3.427 nm^{-1}, and q=1.13, 2.278, and 3.419 nm^{-1}, respectively, with Bragg indices of 1, 2, and 3, which characterizes the presence of lamellar phases. The lattice parameter was equivalent to 5.52 and 5.56 nm for −30°C and −18°C, respectively. Also observed was a decrease in peak width at −18°C compared to those at −30°C. These structural changes of the lamellar domains upon heating may have been related to the appearance of the slight endothermic peak observed at −25°C in a DSC curve. In addition, two broad peaks were observed at q=1.577 and 2.811 at −30°C, and at q=1.577 and 2.827 at −18°C, with Bragg indices 1 and √3, which characterizes the presence of hexagonal phases. The lattice parameter was 3.98 nm for both temperatures. Moreover, a peak identified at q=4.635 nm^{-1} at both temperatures was attributed to the buffer salt crystals, as shown by control analysis (data not shown). With regard to SAXS patterns acquired at 20°C, peaks were identified at q=1.586 and 2.861 nm^{-1} (Bragg indices 1 and √3), indicating only the existence of a hexagonal phase of DOPE. The lattice parameter found was 3.96 nm. Therefore, the DSC peak observed at 12°C (Figure 3A) could have been related to the lamellar to hexagonal (H_{II}) phase transition.

After analysis of the thermal behavior of the DOPE:CHEMS:HBS mixture (Figure 3C), two peaks centered at −3°C and 20°C could be observed. The exothermic DSC peak observed at −3°C was attributed to the crystallization of CHEMS molecules that had not been incorporated into the liposomal membrane. An exothermic peak was also observed in the DSC analysis of pure CHEMS, where the peak was centered at 0°C (data not shown). The decrease in temperature of this crystallization might have been related to the presence of HBS salts, which can interact with CHEMS molecules. SAXS measurements obtained at −25°C and 7°C (Figure 3D) revealed the presence of peaks at q=1.214, 2.743, and 3.588 nm^{-1} and q=1.223, 2.608, and 3.689 nm^{-1}, respectively, which characterizes the lamellar phase of DOPE molecules with Bragg indices of 1, 2, and 3. The lattice parameters found were 5.18 and 5.14 nm, respectively. This structural dimension of the lamellar phase was in agreement with data reported in previous studies for liposomes also composed of DOPE and CHEMS.[29,30] Also identified were SAXS peaks at q=1.544 and 2.870 nm^{-1} and 1.552 and 2.853 nm^{-1} at −25°C and 7°C, respectively, with Bragg indices of 1 and √3, showing the presence of a hexagonal phase of DOPE molecules with lattice parameters equivalent to 4.07 and 4.05 nm. The coexistence of lamellar and hexagonal phases may have been the result of a heterogeneous distribution of CHEMS molecules between the DOPE molecules in the lipid bilayer. The absence of CHEMS among DOPE molecules, in some regions, could have allowed DOPE molecules to be brought close to each other, thus favoring hexagonal phase formation. Another SAXS

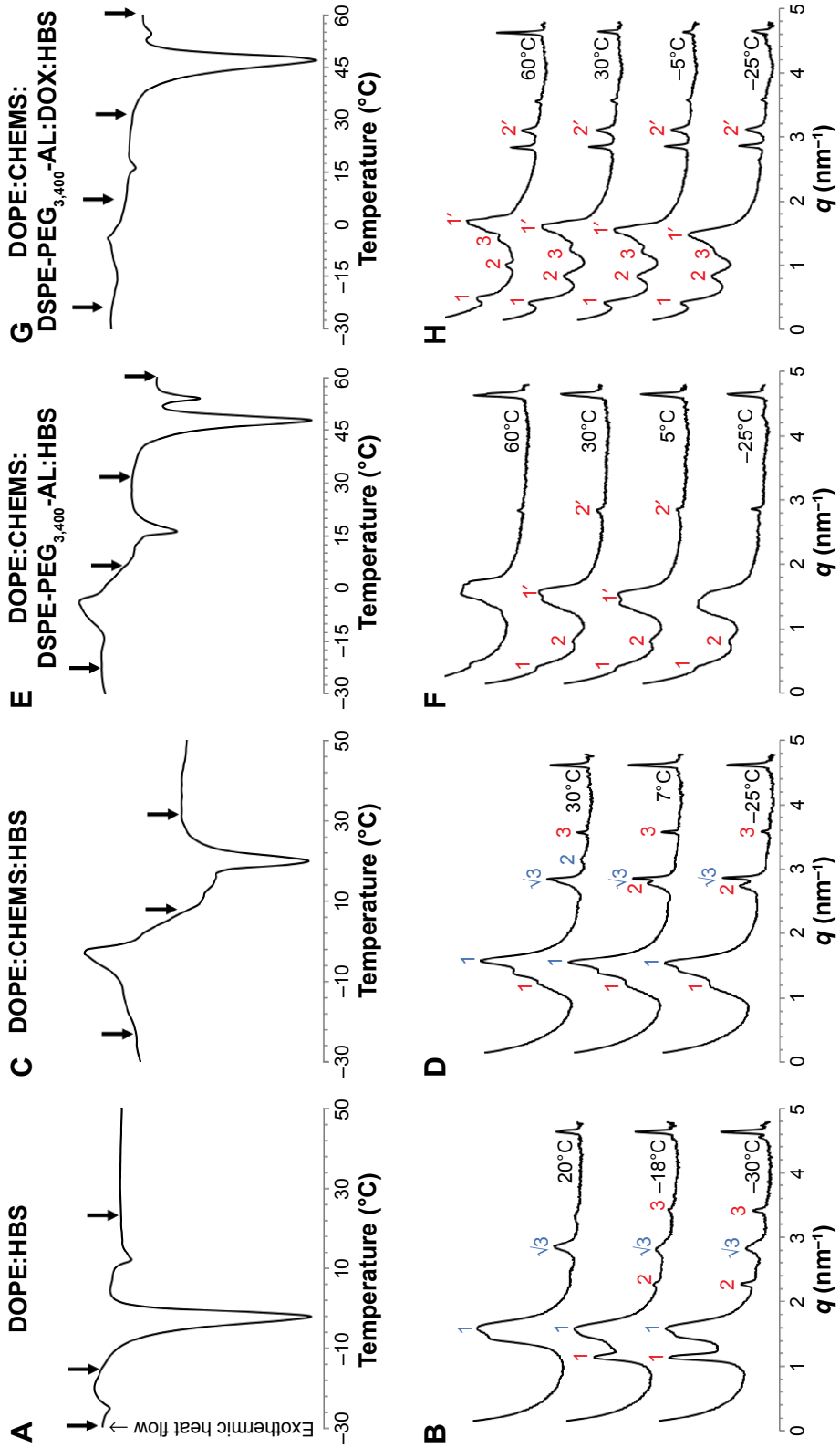

Figure 3 DSC curves and SAXS patterns of lipid mixtures.

Notes: DSC curves of samples DOPE:HBS (**A**), DOPE:CHEMS:HBS (**C**), DOPE:CHEMS:DSPE-PEG$_{3,400}$-AL:HBS (**E**), and DOPE:CHEMS:DSPE-PEG$_{3,400}$-AL:DOX:HBS (**G**), and SAXS patterns at variable temperatures of samples DOPE:HBS (**D**), DOPE:CHEMS:HBS (**B**), DOPE:CHEMS:DSPE-PEG$_{3,400}$-AL:HBS (**F**), and DOPE:CHEMS:DSPE-PEG$_{3,400}$-AL:DOX:HBS (**H**). The indices of SAXS patterns represent the periodicity of the Bragg reflections. Red indices are related to lamellar phases, while blue indices are related to hexagonal phases. Arrows show the temperature in which the SAXS patterns were acquired.

Abbreviations: DSC, differential scanning calorimetry; SAXS, small-angle X-ray scattering; DOPE, 1,2-dioleoyl-glycero-3-phosphatidylethanolamine; HBS, HEPES-buffered saline; HEPES, 4-(2-hydroxyethyl)-1-piperazineethanesulfonic acid; CHEMS, cholesteryl hemisuccinate; DSPE-PEG$_{3,400}$-NHS, 1,2-distearoyl-*sn*-glycero-3-phosphoethanolamine-*N*-(*N*-hydroxysuccinimide-[polyethylene glycol]-3,400); AL, alendronate; DOX, doxorubicin.

peak at q=1.426 nm^{-1} and q=1.400 nm^{-1} at −25°C and 7°C, respectively, was observed, which could not be assigned. The maintenance of the SAXS diffraction pattern for both temperatures indicated that the DSC peak observed at −3°C was not related to any alteration in the structural organization of the lipid membrane. This result confirms that this peak can be related to the crystallization of CHEMS molecules that are not inserted into the lipid membrane. SAXS patterns at 30°C showed a decreased intensity of the peaks attributed to the lamellar phase of DOPE molecules. In addition, peaks were observed at q=1.569, 2.844, and 3.157 nm^{-1}, with periodicity of the Bragg reflections equal to 1, √3, and 2, indicating the presence of the hexagonal phase of DOPE molecules with a lattice parameter equivalent to 4 nm. Since the coexistence of lamellar and hexagonal phases was maintained at 30°C, the endothermic peak observed at 20°C in the DSC curve can be attributed to the melting of free CHEMS molecules. Previous studies also showed the occurrence of this event in mixtures composed of DOPE and CHEMS.[29]

DSC analysis of the DOPE:CHEMS:DSPE-PEG$_{3,400}$-AL:HBS sample is presented in Figure 3E. DSC peaks can be observed centered at −5°C, 16°C, 48°C, and 54°C. The exothermic and endothermic DSC peaks at −5°C and 16°C can be attributed to CHEMS crystallization and melting, respectively, as mentioned earlier. At −25°C, SAXS patterns (Figure 3F) showed peaks at q=0.403 and 0.817 nm^{-1}, with periodicity of the Bragg reflections equal to 1 and 2, which characterizes the presence of the lamellar phase and lattice parameter of 15.59 nm. The increased thickness of the lipid bilayer might have been associated with the presence of DSPE-PEG$_{3,400}$-AL molecules. The insertion of PEG derivatives has been shown to increase bilayer thickness, which can reach up to 15 nm depending on PEG conformation.[31,32] Also identified was a broad peak located in the q-range of 1–1.8 nm^{-1} and a sharp peak at q=2.861 nm^{-1}, for which it was impossible to establish the ratio of Bragg reflections. These peaks were certainly related to a second lamellar system, which developed upon heating and could be clearly identified at 5°C and 30°C. Diffraction patterns at 5°C also showed peaks at q=0.394 and 0.791 nm^{-1} (periodicity of Bragg reflections 1 and 2), which can be associated with lamellar regions with higher amounts of DSPE-PEG$_{3,400}$-AL molecules. The SAXS peaks related to the second lamellar system became clearer, showing peaks located at q=1.392 and 2.853 nm^{-1}. The lattice parameter was 4.51 nm. The observation of two lamellar domains may have been the result of a heterogeneous distribution of DSPE-PEG$_{3,400}$-AL molecules located along the lipid bilayer. At 30°C, diffraction patterns similar to those observed at 5°C were identified, which confirms that the peak observed at 16°C in the DSC curve was not related to alterations in the lipid-bilayer organization. Finally, at 60°C, the second SAXS peak related to the lamellar region enriched in DSPE-PEG$_{3,400}$-AL molecules disappeared, a result that can be explained by the melting of DSPE-PEG$_{3,400}$-AL chains. Therefore, the DSC peaks at 48°C and 54°C can be attributed to this melting of DSPE-PEG$_{3,400}$-AL molecules. DSC analysis of DSPE-PEG$_{3,400}$-AL alone also demonstrated two peaks in this temperature range, confirming the aforementioned proposition (data not shown). Moreover, a broadening of the peak was observed in the q-range of 1.2–1.8 nm^{-1}, which might have been a result of the formation of less ordered structures of DOPE molecules upon heating.

Finally, the influence of the addition of DOX on the thermal behavior of the lipid mixture was investigated. DSC peaks of the DOPE:CHEMS:DSPE-PEG$_{3,400}$-AL:DOX:HBS were observed centered at −4°C, 16°C, 46°C, and 54°C (Figure 3G). The exothermic and endothermic DSC peaks at −4°C and 16°C can be attributed to the crystallization and melting of CHEMS molecules, respectively, as mentioned earlier. In addition, the DSC peaks at 46°C and 54°C can be attributed to the melting of the DSPE-PEG$_{3,400}$-AL molecules, as also described earlier. SAXS analyses at various temperatures were performed in an attempt to confirm this hypothesis (Figure 3H). At −25°C, SAXS peaks were identified at q=0.412, 0.834, and 1.214 nm^{-1}, with periodicity of the Bragg reflections equal to 1, 2, and 3, which are related to the lipid-bilayer region enriched in the DSPE-PEG$_{3,400}$-AL molecules. The lattice parameter was 15.25 nm. Besides, peaks at q=1.476 and 3.115 nm^{-1} were identified (periodicity of Bragg reflections 1 and 2, lattice parameter 4.26 nm), attributed to the lamellar phase of the DOPE molecules. The peaks observed at q=2.869 and 3.596 nm^{-1} might have been related to the DOX crystals. It is noteworthy that these peaks were observed at all temperature intervals investigated. Finally, the SAXS peak at q=4.652 nm^{-1} can be attributed to the buffer salt crystals. At 5°C, the SAXS peaks associated with the two lamellar systems were observed at q=0.412, 0.826, and 1.214 nm^{-1}, and q=1.561 and 3.106 nm^{-1}. The lattice parameters were 15.25 and 4.03 nm, respectively. Similar profiles were obtained for the SAXS patterns at 30°C, showing peaks at q=0.412, 0.834, and 1.248 nm^{-1} (lattice parameter 15.25 nm) and at q=1.611 and 3.106 nm^{-1}, with a lattice parameter of 3.9 nm. At 60°C, the SAXS peaks of both lamellar regions shifted to higher q-values: 0.496, 1.003, and 1.417 nm^{-1} and

1.687 and 3.115 nm^{-1}, respectively. The lattice parameters were 12.67 and 3.72 nm, respectively. The decrease in the value of the lattice parameter can be explained by the melting of the DSPE-$PEG_{3,400}$-AL molecules, leading to higher fluidity of the lipid bilayer. The results described evidenced the occurrence of interactions between the DOX molecules and the lipids forming the long-circulating SpHL-AL. The SAXS patterns of the sample containing DOX molecules were different from those obtained for the sample without DOX molecules at all temperatures evaluated. The presence of DOX molecules allowed a greater structural organization of lipids in two lamellar systems (regions enriched or not in DSPE-$PEG_{3,400}$-AL molecules). This finding may have been the result of the occurrence of electrostatic interactions between the amino group of DOX molecules and the phosphate group of DOPE, DSPE-$PEG_{3,400}$, or DSPE-$PEG_{3,400}$-AL molecules and/or the carboxylic group of CHEMS molecules. It is important to note that the lamellar to nonlamellar phase transitions of DOPE did not occur until 60°C. This result suggests that SpHL-AL-DOX may present good stability against changes in room temperature.

In vitro drug release in HBS, serum, and plasma

Formulations were submitted to leakage studies by means of dialysis against HBS pH 7.4 or 5 (Figure 4A). For SpHL-AL-DOX at pH 7.4, a biphasic release of DOX was observed, with 17% released in the first 8 hours, followed by slow leakage up to 48 hours (~28% released). At pH 5, the release profile was polyphasic, with faster leakage of DOX in the first 3 hours (~40% released), followed by a sustained release up to 24 hours (~52% released). From 24 to 36 hours, the leakage rate increased, followed by a new sustained release up to 48 hours (~88% released). The release profile for SpHL-DOX was similar to the AL-coated formulation, although the total amount of leaked DOX was higher. At pH 7.4, around 22% of the content was leaked in the first 8 hours, followed by a reduction in release rate up to 48 hours (~36% released). At pH 5, a biphasic release profile was observed, with around 62% of DOX released in the first 6 hours and then a slower release occurring up to 48 hours (~96% released). The more rapid release of DOX from liposomes at pH 5 compared to pH 7.4 can be explained by the destabilization of the lipid bilayer under an acidic environment, and proves the pH sensitivity of the formulation. For both formulations (SpHL-AL-DOX and SpHL-DOX) in both conditions (pH 7.4 and 5), a higher DOX-leakage rate was observed at the initial time, which can be related to the release of the drug electrostatically associated with the surface of the liposomes. The subsequent drug release was relatively slow up to 48 hours. The diffusion of DOX through the lipid system might have been responsible for this late-release profile. Studies performed by Garbuzenko et al, using nontargeted pH-sensitive liposomes (SpHLs) containing a radiolabeled peptide, showed a similar release profile.[31] It is noteworthy that the AL molecules attached to the extremity of DSPE-$PEG_{3,400}$ did not destabilize the lipid bilayer, since the release profile was similar for SpHL-AL-DOX and SpHL-DOX. In addition, the interaction between

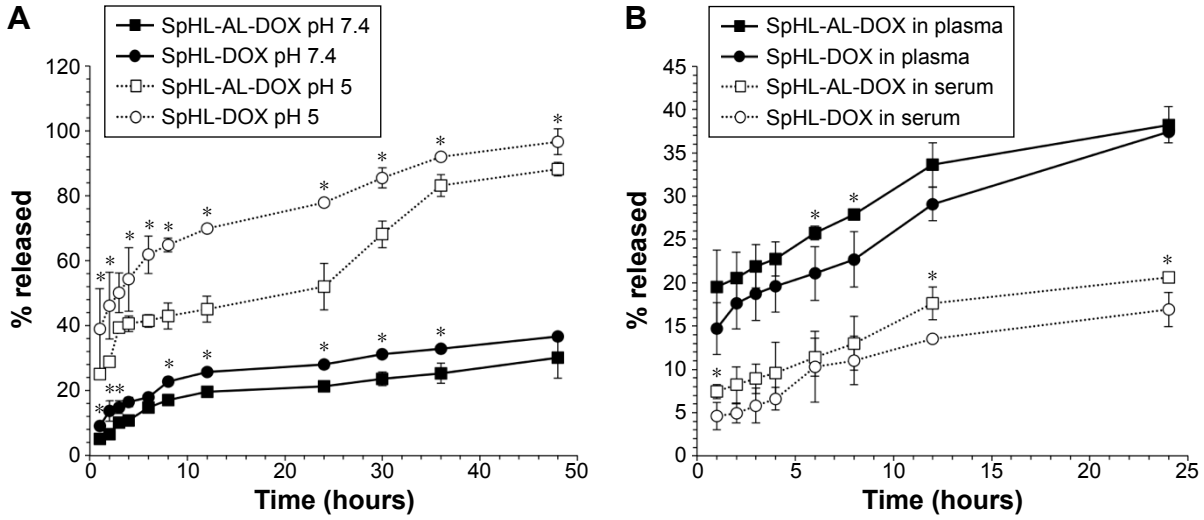

Figure 4 Release profile of DOX from SpHL-AL-DOX or SpHL-DOX in HBS pH 7.4 and 5 (**A**) or plasma and serum (**B**).
Notes: *Significant differences between SpHL-DOX and SpHL-AL-DOX formulations at same pH and time interval, assessed by one-way ANOVA followed by Tukey's HSD test ($P<0.05$). Results expressed as mean ± SEM (n=3).
Abbreviations: DOX, doxorubicin; SpHL-AL-DOX, alendronate-coated long-circulating pH-sensitive liposomes containing DOX; HBS, HEPES-buffered saline; HEPES, 4-(2-hydroxyethyl)-1-piperazineethanesulfonic acid; ANOVA, analysis of variance; HSD, honest significant difference; SEM, standard error of mean.

the DOX molecules and the lipid bilayer, as suggested by the SAXS studies, may explain the slower release of the DOX molecules from SpHL-AL-DOX compared to the AL-uncoated ones. For both formulations, at pH 7.4 the mean diameter and PDI were evaluated prior to and after the release studies, and no difference was observed (Table 4), which confirms the maintenance of membrane stability throughout the time interval. Due to the formation of aggregates at pH 5, it was not possible to measure the mean diameter of these formulations.

For plasma and serum stability, both formulations (SpHL-DOX and SpHL-AL-DOX) were mixed with rat-blood plasma or serum and then submitted to dialysis against HBS pH 7.4 (Figure 4B). The DOX-release profile was similar for both formulations. In plasma, DOX was rapidly leaked from both formulations in the first hour (14.7% and 19.5% for SpHL-DOX and SpHL-AL-DOX, respectively); after that, the release rate remained constant throughout. In serum, the leakage rate was kept constant until 24 hours of analysis. After 24 hours, the leakage percentage was around 35% for both formulations in plasma, and 17% for SpHL-DOX and 20% for SpHL-AL-DOX in serum. The highest amount of DOX released in plasma could be explained by the presence of fibrinogen and the anticoagulant ethylenediaminetetraacetic acid (EDTA) into the medium. It is known that DOX molecules can interact with EDTA molecules to form a poorly water-soluble salt.[33] EDTA, which was added to the blood during the plasma-separation process, interacted with DOX molecules present on the liposomal membrane, promoting its rapid release at initial time. Besides that, it is well known that liposomal formulations can interact with plasma proteins through adsorption or extraction of liposomal membrane components. This interaction can lead to destabilization of the liposomes, associated with the rapid release of the internal content.[33] It is known that plasma possesses a higher protein content, due to the presence of fibrinogen, which could lead to an enhanced destabilization process. In spite of this difference, in this study a slow and constant release of DOX was observed from the liposomes in both blood components, which could have been related to a low interaction between the liposomal membrane and plasma or serum components. This effect can be reached through the insertion of PEG derivatives that generate a steric barrier around the liposomal membrane, avoiding the approaching proteins.[13] After 24 hours, the size of the formulations was determined again (Table 4). The mean diameter and PDI of the formulations had changed slightly, which could indicate initial destabilization. In spite of that, the final mean diameter and PDI were still considered suitable for these types of formulation.

In vitro assessment of HA-binding affinity

The affinity of the liposomes for HA is shown in Figure 5A. Both SpHL-AL-DOX and SpHL-DOX showed weak binding to HA at the initial time point (<1%). After 2 hours, SpHL-DOX kept their low affinity for HA (<5% of binding), whereas SpHL-AL-DOX presented significantly higher affinity (~40% of binding). The highest affinity of SpHL-AL-DOX for HA indicates that the AL molecules were able to attach to the liposomal surface without loss of affinity for HA. Similar results have been reported for the incorporation of other bisphosphonate derivatives in liposomes and other types of nanoparticles, eg, bovine serum albumin, gold, and synthetic polymers.[8–10,34–36] Besides that, the binding percentage of SpHL-AL-DOX was maintained up to 6 hours, which suggests that liposome binding to HA was not time-dependent.

In an attempt to evaluate the strength of binding of SpHL-AL-DOX to HA, the sample submitted to the previous study was submitted to liposomal release-rate evaluation (Figure 5B).

Table 4 Mean diameter and PDI of formulations submitted to release studies

Formulation	Medium	Size (nm)			PDI		
		0 hour	24 hours	48 hours	0 hour	24 hours	48 hours
SpHL-DOX	HBS	173±13	161±18	161±10	0.08±0.02	0.10±0.01	0.07±0.02
	Serum	160±8	181±10*	–	0.09±0.01	0.17±0.04*	–
	Plasma	165±5	176±5*	–	0.07±0.02	0.15±0.05*	–
SpHL-AL-DOX	HBS	148±6	153±11	160±6	0.08±0.03	0.11±0.02	0.13±0.03
	Serum	132±7	158±6*	–	0.07±0.02	0.21±0.06*	–
	Plasma	136±10	164±2*	–	0.09±0.02	0.17±0.03*	–

Notes: *Significant differences between the time analyzed and initial time for the same formulation at the same medium, as assessed by *t*-test ($P<0.05$). Values expressed as mean ± SD (n=3).

Abbreviations: PDI, polydispersity index; SpHL-DOX, pH-sensitive liposomes containing doxorubicin (long-circulating); AL, alendronate; SpHL-AL-DOX, AL-coated SpHL-DOX; HBS, HEPES-buffered saline; HEPES, 4-(2-hydroxyethyl)-1-piperazineethanesulfonic acid; SD, standard deviation.

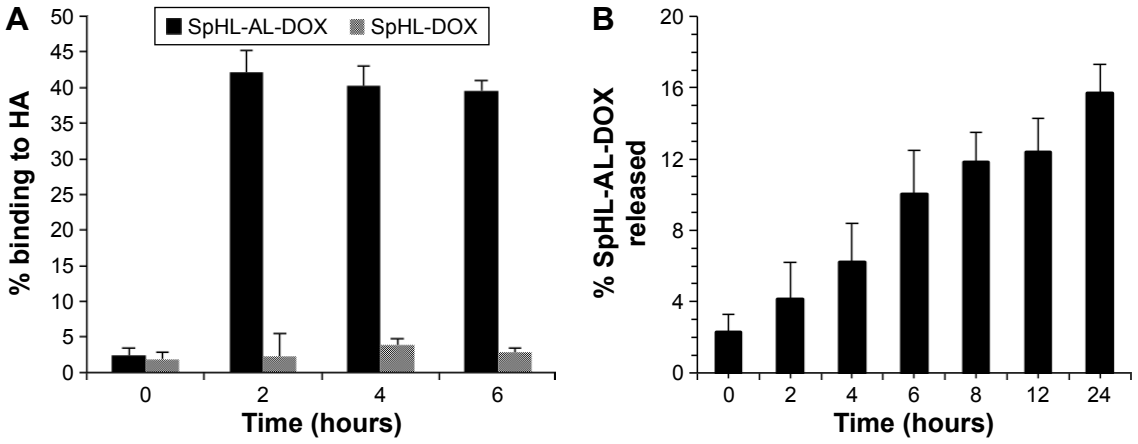

Figure 5 Degree of binding of SpHL-AL-DOX and SpHL-DOX to HA (**A**) and release profile of SpHL-AL-DOX after association with HA (**B**).
Note: Results expressed as mean ± SEM (n=3).
Abbreviations: SpHL-AL-DOX, alendronate-coated long-circulating pH-sensitive liposomes containing doxorubicin; HA, hydroxyapatite; SEM, standard error of mean.

The release rate of SpHL-AL-DOX from HA was nearly constant throughout the evaluated time interval. The amount of phosphorus in the dispersant phase varied from 2% to 16% of the total of the liposomes during the first 24 hours, indicating strong binding of SpHL-AL-DOX to HA. The strong binding to HA is essential to obtain prolonged liposomal retention in bones. These results indicate that the liposomes are able to interact specifically with HA through the complexation of phosphonate groups with Ca^{2+} ions.

Cytotoxicity assay

Cell viability of free DOX or SpHL-AL-DOX was determined using MDA-MB-231 cells and compared to untreated cells. Free DOX and SpHL-AL-DOX had a similar cytotoxic effect, and induced significant dose-dependent effects (Figure 6). IC_{50} values were 120±15 and 153±20 nmol·L^{-1} for free DOX and SpHL-AL-DOX, respectively. These results were not significantly different ($P>0.05$). Similar results for both free and encapsulated DOX can be explained by the destabilization of the liposomal membrane after cell internalization. The acidification of the endosome leads to the protonation of carboxylate groups of CHEMS molecules, which suppress charge repulsion within the lipid bilayer, inducing the reversion of DOPE molecules into their inverted hexagonal phase. Consequently, this effect promotes the liposome destabilization or fusion with the endosome and allows the release of DOX into the tumor-cell cytoplasm.[37] Blank liposomes (SpHL-AL) were also tested under the same dilutions used for SpHL-AL-DOX, and no cytotoxicity to the tumor cells was observed in the concentration range studied, showing that the cytotoxicity of SpHL-AL-DOX was related specifically to the action of DOX in the tumor cells.

Biodistribution studies

DOX content was quantified in each organ and calculated as percentage of injected dose per gram of tissue (Figure 7).

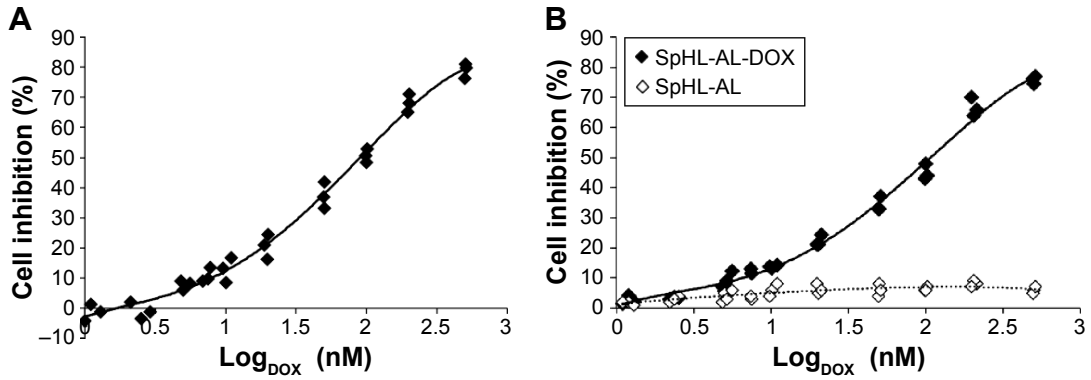

Figure 6 MDA-MB-231 cell-inhibition curves after 48 hours' incubation with free DOX (**A**) or SpHL-AL-DOX (**B**).
Notes: Blank liposomes (SpHL-AL) were submitted to the same dilution of SpHL-AL-DOX, and inhibition curves represent the effect of the formulation alone for each dilution of SpHL-AL-DOX.
Abbreviations: DOX, doxorubicin; SpHL-AL-DOX, alendronate-coated long-circulating pH-sensitive liposomes containing DOX.

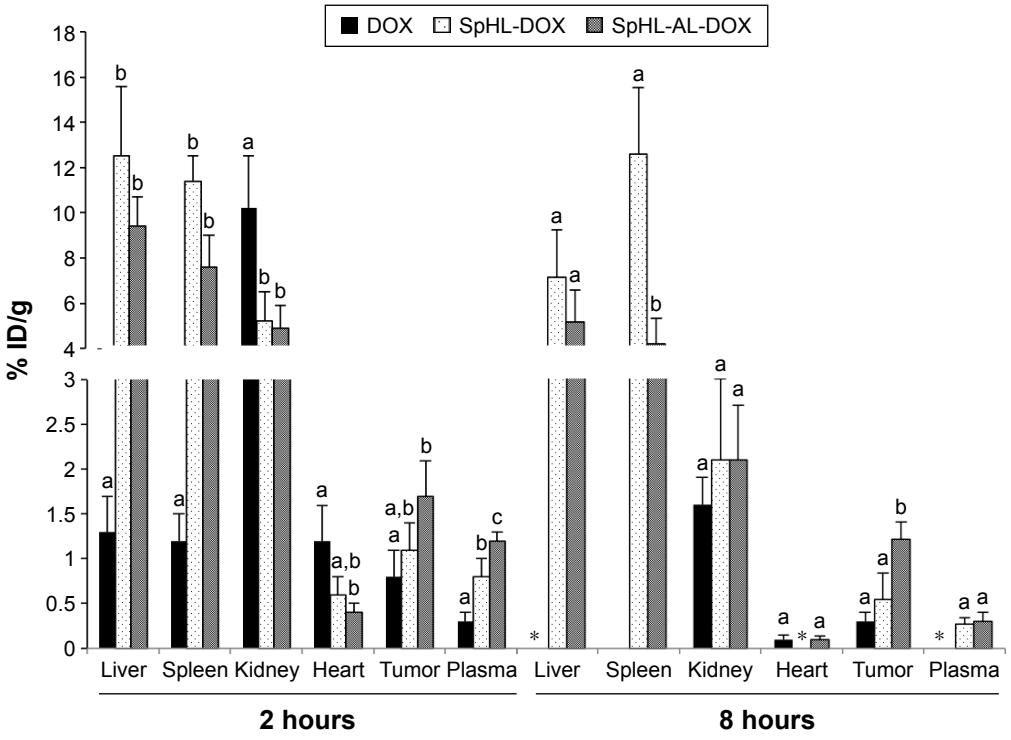

Figure 7 Biodistribution profile of free DOX, SpHL-DOX, and SpHL-AL-DOX at 2 or 8 hours postinjection in female nude BALB/c mice bearing MDA-MB-231 bone metastasis.

Notes: Different letters indicate significant differences between treatment groups for the same organ at the same time interval, assessed by one-way ANOVA followed by Tukey's HSD test ($P<0.05$). Results expressed as mean ± SEM (n=3). *Represents the organs in which the concentration of DOX was undetectable.

Abbreviations: DOX, doxorubicin; SpHL-DOX, long-circulating pH-sensitive liposomes containing DOX; SpHL-AL-DOX, alendronate-coated SpHL-DOX; ID, injected dose; ANOVA, analysis of variance; HSD, honest significant difference; SEM, standard error of mean.

For the free DOX group, an intense uptake of DOX by kidneys was observed at 2 hours postinjection, and after 8 hours the amount was reduced sixfold, indicating rapid clearance of the drug. The reduction in kidney uptake was followed by complete elimination of DOX from the bloodstream. Other organs presented relatively lower drug uptake for both time intervals. Also noteworthy was the higher uptake of free DOX into heart and tumor tissue at 2 hours when compared to blood. The uptake of DOX into the heart can be explained by the fact that this cationic drug was retained in the mitochondrial inner membrane by forming a nearly irreversible complex with cardiolipin. Since cardiac muscle presents high respiratory activity, mitochondria are prevalent in this area.[38] This fact is one of the bases to explain cardiac toxicity caused by DOX. The proteins of the electron-transport chain require cardiolipin binding to function properly, and it has been argued that since DOX disrupts the cardiolipin–protein interface, superoxide (O_2^-) formation occurs, injuring the myocardium.[39]

For the liposomal DOX, both formulations showed significant uptake by the liver and spleen, as nanostructures are normally trapped by macrophages present in these organs.[40] High renal excretion was also observed. Other organs evaluated presented significantly lower uptake in the whole experiment. The heart uptake of DOX was significantly reduced for both liposomes at 2 hours postinjection when compared to the free drug. At 8 hours postinjection, the values were reduced significantly, approaching zero. In the bloodstream, a higher concentration of the drug was observed for both liposomes at 2 and 8 hours, indicating that the drug circulated for a longer time when encapsulated in the liposomes. In parallel, uptake in the tumor area at 2 hours was increased for the SpHL-AL-DOX treatment. The retention of DOX in the tumor area was also longer for this treatment group when compared to the other, being equal to four times and twice as concentrated than free DOX or SpHL-DOX, respectively.

Upon evaluation of the tumor:bloodstream ratio at 2 hours, values of 2.7±0.4, 1.4±0.3, and 1.4±0.2 were observed for free DOX, SpHL-DOX, and SpHL-AL-DOX, respectively. The lower values observed for both liposomes can be explained by the longer circulation time achieved by these formulations, which increases the concentration of the drug in the bloodstream. On the other hand, when this ratio was calculated at 8 hours, an important increment

was observed in the tumor affinity for SpHL-AL-DOX (tumor:bloodstream ratio 3.9±0.6) when compared to SpHL-DOX (tumor:bloodstream ratio 2±0.4). For the free DOX, it was not possible to calculate this value, since the drug concentration in the blood was undetectable. These results show the capacity of SpHL-AL-DOX to interact and be retained in the tumor site.

The longer circulation time, higher tumor uptake, and reduced heart uptake for the liposomal formulations when compared to the free drug can be explained by two factors: 1) the size of the liposomes, which made the DOX less susceptible to be taken up by healthy tissues, such as the myocardium; and 2) the encapsulation of DOX in long-circulating liposomes, which allowed its retention for a long time in the bloodstream, enhancing its ability to reach the tumor area and be taken up due to the EPR effect.[41] Also, the higher uptake of DOX in the tumor area and the lower uptake in the heart after SpHL-AL-DOX treatment when compared to SpHL-DOX treatment can be explained by the presence of AL on the liposomal surface, which allowed for the interaction of this formulation with the local bone matrix, with increased release of DOX in that area.[42]

Conclusion

DSC and SAXS results evidenced the occurrence of interaction between the DOX molecules and the liposomal membrane, leading to a more organized bilayer structure. Further studies aiming to better understand these interactions and their effects on the physicochemical and biological behavior of liposomal formulations will be useful for planning the development of new DOX liposomal formulations. The formulation developed in this work (SpHL-AL-DOX) accomplished four essential aspects of its purpose: 1) it demonstrated suitable plasma and serum stability, which are essential to maintain the drug protected in the aqueous phase of liposomes, avoiding uptake by healthy tissues; 2) the high affinity and capacity for holding the encapsulated drug in the tumor area can be guaranteed by the active targeting provided by the insertion of DSPE-$PEG_{3,400}$-AL, which demonstrated a strong interaction with HA; 3) since SpHL-AL-DOX would be able to be taken up in the tumor region, the extra- and/or intracellular release of DOX could be achieved by the demonstrated pH sensitivity; and 4) the maintenance of the cytotoxicity against breast cancer tumor cells shows that the encapsulated drug is not prevented from acting after reaching the tumor area. These results demonstrate the potential of this formulation as a rational tool for further studies of efficacy and toxicity against breast cancer metastases in bones.

Acknowledgments

The authors would like to thank Fundação de Amparo à Pesquisa do Estado de Minas Gerais – FAPEMIG (REDE-40/11) and Conselho Nacional de Desenvolvimento Científico e Tecnológico – CNPq (306197/2014-6) for the financial support. The authors thank Dr Mateus Borba Cardoso and his staff for their competence and support during the measurements at Laboratório Nacional de Luz Síncrotron – LNLS (Campinas, Brazil). The authors also thank Fundação Coordenação de Aperfeiçoamento de Pessoal de Nível Superior – CAPES for supporting DSF with a scholarship. PC acknowledges the National Institutes of Health for generous research and instrumentation support (R01EB009062, S10OD010650).

Author contributions

DSF was responsible for conducting and analyzing the results of the experiments performed. The following authors were responsible for conducting and analyzing the results in partnership with DSF on specified experiments: SDF and LAMF on the development and physicochemical characterization of formulations; SCAL, AM, and RMP on SAXS studies; CST on cytotoxicity studies; JDSF and RJA on synthesis and characterization of DSPE-$PEG_{3,400}$-AL; and BLJPO on the stability and HA-affinity studies. ASRG and PC advised and financially supported the experiments performed at Massachusetts General Hospital, and MCO coordinated the project and financially supported the experiments performed at Universidade Federal de Minas Gerais. All authors contributed toward data analysis, drafting and critically revising the paper and agree to be accountable for all aspects of the work.

Disclosure

The authors report no conflicts of interest in this work.

References

1. Harvey HA, Cream LR. Biology of bone metastases: causes and consequences. *Clin Breast Cancer*. 2007;7(Suppl 1):S7–S13.
2. Li S, Peng Y, Weinhandl ED, et al. Estimated number of prevalent cases of metastatic bone disease in the US adult population. *Clin Epidemiol*. 2012;4:87–93.
3. Liede A, Jerzak KJ, Hernandez RK, Wade SW, Sun P, Narod SA. The incidence of bone metastasis after early-stage breast cancer in Canada. *Breast Cancer Res Treat*. 2016;156:587–595.
4. Shea J, Miller S. Skeletal function and structure: implications for tissue-targeted therapeutics. *Adv Drug Deliver Rev*. 2005;57:945–957.
5. Bergmann R, Meckel M, Kubicek V, et al. ^{177}Lu-labelled macrocyclic bisphosphonates for targeting bone metastasis in cancer treatment. *EJNMMI Res*. 2016;6:5.
6. Yewle JN, Puleo DA, Bachas LG. Bifunctional bisphosphonates for delivering PTH (1 – 34) to bone mineral with enhanced bioactivity. *Biomaterials*. 2013;34:3141–3149.
7. Yang Y, Bhadari KH, Panahifar A, Doschak MR. Synthesis, characterization and biodistribution studies of ^{125}I-radioiodinated di-PEGylated bone targeting salmon calcitonin analogue in healthy rats. *Pharm Res*. 2013;31:1146–1157.

8. Anada T, Takeda Y, Honda Y, Sakurai K, Suzuki O. Synthesis of calcium phosphate-binding liposome for drug delivery. *Bioorg Med Chem Lett*. 2009;19:4148–4150.
9. Farbod K, Diba M, Zinkevich T, et al. Gelatin nanoparticles with enhanced affinity for calcium phosphate. *Macromol Biosci*. 2016;16:717–729.
10. Swami A, Reagan MR, Basto P, et al. Engineered nanomedicine for myeloma and bone microenvironment targeting. *Proc Natl Acad Sci U S A*. 2014;111:10287–10292.
11. Roelofs A, Thompson K, Gordon S, Rogers M. Molecular mechanisms of action of bisphosphonates: current status. *Clin Cancer Res*. 2006;12:6222s–6230s.
12. Ferreira D, Lopes S, Franco M, Oliveira M. pH-sensitive liposomes for drug delivery in cancer treatment. *Ther Deliv*. 2013;4:1099–1123.
13. Torchilin V. Multifunctional and stimuli-sensitive nanoparticulate system for drug delivery. *Nat Rev Drug Discov*. 2014;13:813–827.
14. Bangham A, Standish M, Watkins J. Diffusion of univalent ions across the lamellae of swollen phospholipids. *J Mol Biol*. 1965;13:238–255.
15. Barenholz Y. Liposome application: problems and prospects. *Curr Opin Colloid Interface Sci*. 2001;6:66–77.
16. Ananchenko G, Novakovic J, Tikhomirova A. Alendronate sodium. In: Brittain HG, editor. *Profiles of Drug Substances, Excipients, and Related Methodology*. Vol 38. San Diego: Elsevier; 2013:1–34.
17. Chmelík M, Valkovič L, Wolf P, et al. Phosphatidylcholine contributes to in vivo ^{31}P MRS signal from the human liver. *Eur Radiol*. 2015;25:2059–2066.
18. Klykov O, Weller MG. Quantification of N-hydroxysuccinimide and N-hydroxysulfosuccinimide by hydrophilic interaction chromatography (HILIC). *Anal Methods*. 2015;7:6443–6448.
19. Pattni BS, Chupin VV, Torchilin VP. New developments in liposomal drug delivery. *Chem Rev*. 2015;115:10938–10966.
20. Bolkestein M, de Blois E, Koelewijn SJ, et al. Investigation of factors determining the enhanced permeability and retention effect in subcutaneous xenografts. *J Nucl Med*. 2016;57:601–607.
21. Maeda H, Tsukigawa K, Fang J. A retrospective 30 years after discovery of the enhanced permeability and retention effect of solid tumors: next-generation chemotherapeutics and photodynamic therapy problems, solutions, and prospects. *Microcirculation*. 2016;23:173–182.
22. Kanazaki K, Sano K, Makino A, et al. Feasibility of poly(ethylene glycol) derivatives as diagnostic drug carriers for tumor imaging. *J Control Release*. 2016;226:115–123.
23. Alanne A, Hyvönen H, Lahtinen M, et al. Systematic study of the physicochemical properties of a homologous series of aminobisphosphonates. *Molecules*. 2012;17:10928–10945.
24. Lasic D. Novel applications of liposomes. *Trends Biotechnol*. 1998;16:307–321.
25. Negreira N, Mastroianni N, Alda ML, Barceló D. Multianalyte determination of 24 cytostatics and metabolites by liquid chromatography-electrospray-tandem mass spectrometry and study of their stability and optimum storage conditions in aqueous solution. *Talanta*. 2013;116:290–299.
26. Shibata H, Yomota C, Kawanishi T, Okuda H. Polyethylene glycol prevents in vitro aggregation of slightly negatively-charged liposomes induced by heparin in the presence of bivalent ions. *Biol Pharm Bull*. 2006;33:2081–2087.
27. Johnsson M, Edwards K. Liposomes, disks, and spherical micelles: aggregate structure in mixtures of gel phase phosphatidylcholines and poly(ethylene glycol)-phospholipids. *Biophys J*. 2003;85:3839–3847.
28. Lopes SC, Novais MV, Teixeira CS, et al. Preparation, physicochemical characterization, and cell viability evaluation of long-circulating and pH-sensitive liposomes containing ursolic acid. *Biomed Res Int*. 2013;2013:467147.
29. Lopes SC, Novais MV, Ferreira DS, et al. Ursolic acid incorporation does not prevent the formation of a non-lamellar phase in pH-sensitive and long-circulating liposomes. *Langmuir*. 2014;30:15083–15090.
30. Silva SM, Coelho LN, Malachias A, et al. Study of the structural organization of cyclodextrin-DNA complex loaded anionic and pH-sensitive liposomes. *Chem Phys Lett*. 2011;506:66–70.
31. Garbuzenko O, Barenholz Y, Priev A. Effect of grafted PEG on liposome size and on compressibility and packing of lipid bilayer. *Chem Phys Lipids*. 2005;135:117–129.
32. Varga Z, Wacha A, Vainio U, Gummel J, Bóta A. Characterization of the PEG layer of sterically stabilized liposomes: a SAXS study. *Chem Phys Lipids*. 2012;165:387–392.
33. Song Y, Huang Z, Song Y, et al. The application of EDTA in drug delivery systems: doxorubicin liposomes loaded via NH_4EDTA gradient. *Int J Nanomedicine*. 2014;9:3611–3621.
34. Rudnick-Glick S, Corem-Salkmon E, Grinberg I, Yehuda R, Margel S. Near IR fluorescent conjugated poly(ethylene glycol) bisphosphonate nanoparticles for in vivo bone targeting in a young mouse model. *J Nanobiotechnology*. 2015;13:80.
35. Rawat P, Manglani K, Gupta S, et al. Design and development of bioceramic based functionalized PLGA nanoparticles of risendronate for bone targeting: in-vitro characterization and pharmacodynamics evaluation. *Pharm Res*. 2015;32:3149–3158.
36. Pignatello R, Sarpietro M, Castelli F. Synthesis and biological evaluation of a new polymeric conjugate and nanocarrier with osteotropic properties. *J Funct Biomater*. 2012;3:79–99.
37. Simões S. On the formulation of pH-sensitive liposomes with long circulation times. *Adv Drug Deliv Rev*. 2004;56:947–965.
38. Goormaghtigh E, Huart P, Praet M, Brasseur R, Ruysschaert JM. Structure of the adriamycin-cardiolipin complex: role in mitochondrial toxicity. *Biophys Chem*. 1990;35:247–257.
39. Schlame M, Rua D, Greenberg ML. The biosynthesis and functional role of cardiolipin. *Prog Lipid Res*. 2000;39:257–288.
40. Júnior AD, Mota LG, Nunan EA, et al. Tissue distribution evaluation of stealth pH-sensitive liposomal cisplatin versus free cisplatin in Ehrlich tumor-bearing mice. *Life Sci*. 2007;80:659–664.
41. Ulrich AS. Biophysical aspects of using liposomes as delivery vehicles. *Biosci Rep*. 2002;72:129–150.
42. Ferreira DS, Boratto FA, Cardoso VN, et al. Alendronate-coated long-circulating liposomes containing ^{99m}technetium-ceftizoxime used to identify osteomyelitis. *Int J Nanomedicine*. 2015;10:2441–2450.